PAPER

Magnetism and spin dynamics in roomtemperature van der Waals magnet Fe₅GeTe₂

To cite this article: Laith Alahmed et al 2021 2D Mater. 8 045030

View the article online for updates and enhancements.

You may also like

- Revealing room temperature ferromagnetism in exfoliated Fe₅GeTe₂ flakes with quantum magnetic imaging Hang Chen, Shahidul Asif, Matthew Whalen et al.
- Emerging intrinsic magnetism in twodimensional materials: theory and applications Songrui Wei, Xiaoqi Liao, Cong Wang et
- <u>Magnetic two-dimensional van der Waals</u> <u>materials for spintronic devices</u>
 Yu Zhang, , Hongjun Xu et al.

2D Materials



RECEIVED 8 February 2021

REVISED

12 July 2021

ACCEPTED FOR PUBLICATION 22 August 2021

PUBLISHED

13 September 2021

PAPER

Magnetism and spin dynamics in room-temperature van der Waals magnet Fe₅GeTe₂

Laith Alahmed¹, Bhuwan Nepal², Juan Macy³, Wenkai Zheng³, Brian Casas³, Arjun Sapkota², Nicholas Jones¹, Alessandro R Mazza⁴, Matthew Brahlek⁴, Wencan Jin⁵, Masoud Mahjouri-Samani¹, Steven S.-L. Zhang⁶, Claudia Mewes², Luis Balicas³, Tim Mewes², and Peng Li¹, ®

- Department of Electrical and Computer Engineering, Auburn University, Auburn, AL 36849, United States of America
- Department of Physics, University of Alabama, Tuscaloosa, AL 35487, United States of America
- National High Magnetic Field Laboratory, Florida State University, Tallahassee, FL 32310, United States of America
- ⁴ Materials Science and Technology Division, Oak Ridge National Laboratory, Oak Ridge, TN 37831, United States of America
- Department of Physics, Auburn University, Auburn, AL 36849, United States of America
- Department of Physics, Case Western Reserve University, Cleveland, OH 44106, United States of America
- Department of Physics, Florida State University, Tallahassee, FL 32306, United States of America
- * Authors to whom any correspondence should be addressed.

E-mail: wzj0029@auburn.edu, sxz675@case.edu, balicas@magnet.fsu.edu, tmewes@ua.edu and pzl0047@auburn.edu

Keywords: Fe₃GeTe₂, spin dynamics, room-temperature ferromagnetism, van der Waals magnet Supplementary material for this article is available online

Abstract

Two-dimensional van der Waals (vdWs) materials have gathered a lot of attention recently. However, the majority of these materials have Curie temperatures that are well below room temperature, making it challenging to incorporate them into device applications. In this work, we synthesized a room-temperature vdW magnetic crystal Fe₅GeTe₂ with a Curie temperature $T_c = 332$ K, and studied its magnetic properties by vibrating sample magnetometry (VSM) and broadband ferromagnetic resonance (FMR) spectroscopy. The experiments were performed with external magnetic fields applied along the c-axis (H||c) and the ab-plane (H||ab), with temperatures ranging from 300 to 10 K. We have found a sizable Landé g-factor difference between the H||c| and H||ab| cases. In both cases, the Landé g-factor values deviated from g=2. This indicates contribution of orbital angular momentum to the magnetic moment. The FMR measurements reveal that Fe₅GeTe₂ has a damping constant comparable to Permalloy. With reducing temperature, the linewidth was broadened. Together with the VSM data, our measurements indicate that Fe₅GeTe₂ transitions from ferromagnetic to ferrimagnetic at lower temperatures. Our experiments highlight key information regarding the magnetic state and spin scattering processes in Fe₅GeTe₂, which promote the understanding of magnetism in Fe₅GeTe₂, leading to implementations of Fe₅GeTe₂ based room-temperature spintronic devices.

1. Introduction

The increasing interest in magnetic two-dimensional (2D) van der Waals (vdWs) materials in recent years is warranted by their importance for fundamental studies of 2D magnetism, as well as potential applications for spintronic devices. Compared to three-dimensional (3D) magnets, 2D magnetic materials exhibit exotic electrotransport, optical, and spin properties [1–3]. One of the biggest practical issues of most 2D vdWs magnetic materials is that they generally have a Curie temperature (T_c) that is well below

room temperature, making it difficult to incorporate them into relevant devices [4–9]. For example, the Curie temperatures of 2D magnetic materials such as Cr(Si,Ge)Te₃ (33 and 61 K) [4, 5], and Cr(Br,I)₃ (47 and 61 K) [6, 7], are all lower than typical 3D magnets. This is due to their 2D nature, where the pair-exchange interaction is much weaker than in 3D magnets, as it is mostly mediated by neighboring magnetic atoms in the 2D plane.

The low T_c of the aforementioned 2D vdWs ferromagnets makes it impossible to use them in room-temperature spintronic devices. More specifically, in

the 2D limit, it was shown theoretically that the Curie temperature is given by the uniaxial magnetic anisotropy constant *K*, and the spin-exchange interaction *J*, as follows [10]:

$$T_c \sim \frac{4\pi J}{3\ln(\pi^2 J/K)}.$$
 (1)

According to equation (1), as the magnetic anisotropy in vdWs ferromagnets is much smaller than the exchange interaction, T_c is low [11]. It should be noted that the Fe₅GeTe₂ compound has a complex crystalline structure with more than one inequivalent iron positions. Thus, this equation only gives a crude estimation of T_c . Extensive research efforts succeeded in engineering 2D materials that could overcome these challenges. For example, T_c can be significantly raised to about room temperature by enhancing exchange interaction while keeping the vdWs structure [11], such as in the layered 2D Fe_nGeTe₂ ($n \ge$ 3) [12, 13]. This led to Fe₃GeTe₂ with T_c around 220 K [9, 14, 15], Fe₄GeTe₂ with $T_c = 270$ K [11], and Fe₅GeTe₂ with T_c ranging from 260 to 310 K, depending on the Fe content [13, 16, 17].

Fe₅GeTe₂ was first synthesized by May *et al* who found that its Curie temperature is ~310 K [16, 17]. It was later discovered that Fe₅GeTe₂ possesses itinerant long-range ferromagnetism [13], which originates from the giant spin polarization of the delocalized ligand Te states [18]. A recent work reported that Fe₅GeTe₂ transitions from ferromagnetic to ferrimagnetic at 275 K, and then to glassy clusters as the temperature reduces to 100 K [19]. Besides, several groups carried out electro-transport measurements and detected anomalous and topological Hall effects [19–21]. The magnetization dynamics in Fe₅GeTe₂ however, remain unexplored, and thus, is the focus of this work.

Ferromagnetic resonance (FMR) spectroscopy is an important technique to study magnetization dynamics [22, 23]. Several studies have analyzed the spin dynamics in 2D magnets by FMR [24–26], which revealed their magnetocrystalline anisotropy dependence on temperature. It is found that there is a discrepancy between the Landé g-factor along the caxis and the ab-plane directions in the 2D magnet Cr₂Ge₂Te₆ [26, 27]. However, the Landé g-factor is quite isotropic along different directions in another 2D magnet CrI₃ [25]. These measurements were all performed on 2D magnets with low Curie temperatures (e.g. $T_c = 61$ K for CrI_3). With the most promising room-temperature vdWs magnet arguably being Fe₅GeTe₂, we are interested in understanding its quasi-static and dynamic magnetic properties, which can shed light on its magnetic states and spin scattering mechanisms.

We first synthesize the vdWs magnet Fe₅GeTe₂, and then we study its magnetization properties using both vibrating sample magnetometry (VSM) and FMR spectroscopy, in the temperature range of 300

to 10 K. For FMR, a microwave field was applied to the sample in addition to a quasi-static magnetic field, thus triggering spin precession. At the resonance field H_{res} for a given microwave frequency f, FMR oscillations (uniform-mode excitation with $k \approx 0$) occur. The FMR spectroscopy has revealed different Landé g-factors along the c-axis and the ab-plane in Fe₅GeTe₂, indicative of orbital moment contribution to the magnetic moment. After examining the temperature dependence of the FMR linewidth, we find that Fe₅GeTe₂ has an effective damping coefficient similar to Permalloy at room temperature. The increased FMR linewidth at lower temperatures indicates that Fe₅GeTe₂ experiences a magnetic phase transition from ferromagnetism to ferrimagnetism.

2. Structure characterization

Nominal Fe_5GeTe_2 crystals are grown using a mixture of precursor materials filled into a quartz ampoule that is vacuumed and sealed with 1.9 mg cm⁻³ of iodine as a transport agent. The mixture consists of pure elements of Fe:Ge:Te in the molar ratio of 6.2:1:2 (Fe: 99.998%, powder, Alfa Aesar; Ge: 99.999%, 100 mesh, Alfa Aesar; Te: 99.999%, powder, Alfa Aesar). The excess Fe powder is to compensate for any possible Fesite vacancies that might occur during the growth.

A standard MTI 2-zone model OTF-1200X furnace was employed, where the reactants or elemental precursors were placed in the high-temperature zone and the products were grown in the low-temperature side. The ramping rate for both the hot (775 °C) and cold (700 °C) zones to their target temperatures was 1 °C min $^{-1}$. This temperature differential was held for 14 days with the Fe₅GeTe₂ crystals being subsequently quenched in an ice bath.

Prior to characterization, the excess iodine was removed through a bath and rinse cycle of acetone and isopropyl alcohol, respectively. Samples were either stored in a glove box with high purity argon gas (99.99%) of 0.01 ppm O_2/H_2O , or a desiccator under vacuum with pressures ranging between 100–200 mTorr.

The following results are obtained from a bulk Fe_5GeTe_2 crystal in the shape of an ellipse, with area = 3.2×10^{-3} cm² and thickness ~100 microns. The crystalline structure characterization is presented in figure 1. Figure 1(a) shows the crystal structure schematic of Fe_5GeTe_2 . The vdW-separated eight atomic-thick monolayers of two unit cells can be observed, where the vdWs gaps exist between the Te atoms of neighboring unit cells. The light-blue circles labeled Fe(1) represent the two possible occupation locations for the Fe(1) atoms, either above or below a given Ge atom, with an occupation probability not exceeding 50%, as the Fe–Ge bond becomes non-physical if both locations are occupied simultaneously [16].

2D Mater. **8** (2021) 045030 L Alahmed et al

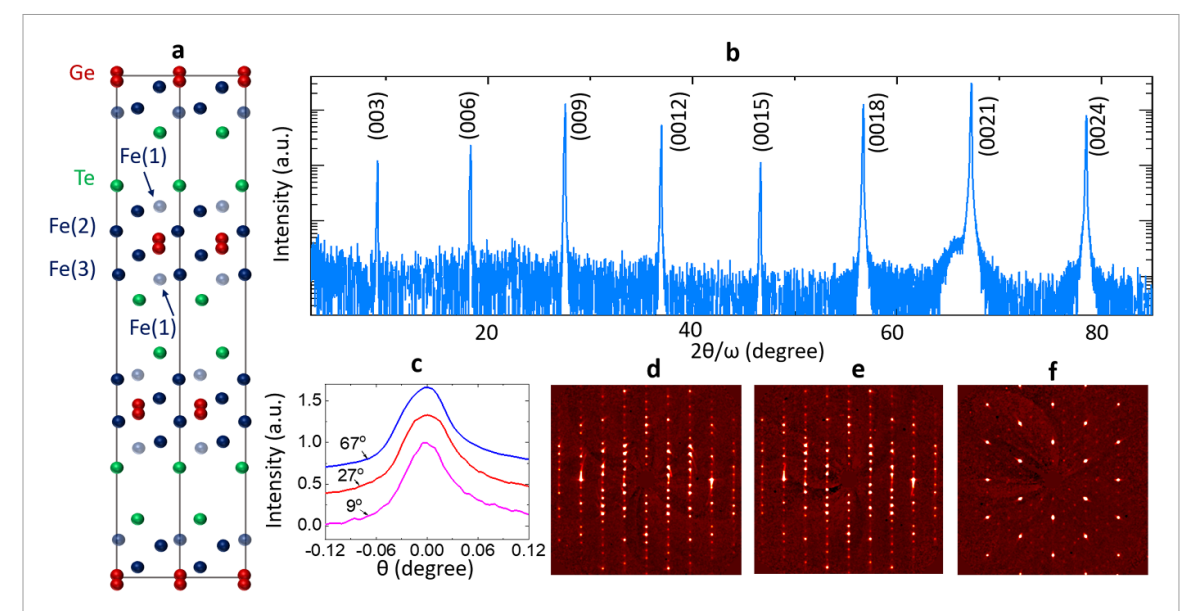


Figure 1. Crystal structure and x-ray diffraction (XRD) of single crystal Fe₅GeTe₂. (a) Schematic of crystal structure of Fe₅GeTe₂. (b) XRD $2\theta/\omega$ scan showing (00*l*) peaks. (c) Rocking curve scan of the peaks at 9°, 27°, 67° showing high crystallinity. (d)–(f) Single crystal XRD scan of Bragg reflections of different planes. (d) (0*kl*) plane. (e) (*h*0*l*) plane. (f) (*hk*0) plane.

The x-ray diffraction (XRD) data collected for the experimental Fe₅GeTe₂ sample crystal are shown in figure 1(b). The (00l) reflections reveal the c-axis of the single crystal. The (00l) peaks, where l=3n, reflect an ABC stacking sequence in the unit cell of the bulk crystal. This is consistent with the rhombohedral lattice structure of the R3m (No. 166) space group, as previously reported [13, 16].

The rocking curves measured at (00l) peak angles are shown in figure 1(c). The full-width-at-half-maximum values of the acquired curves, with values less than 0.06° , reflect the high level of crystallinity of the Fe₅GeTe₂ samples. Figures 1(d)–(f) are Bragg reflection scans of different crystal planes (0kl), (h0l), (hk0) from high-resolution XRD. They all show clear streaks, confirming the high quality of the single-crystal samples.

3. Quasi-static magnetization properties

Quasi-static magnetization properties were measured using VSM in a Quantum Design Dynacool PPMS system. The measurements were carried out with the magnetic field applied along both the c-axis (H||c) and the ab-plane (H||ab) directions. To determine the Curie temperature of the sample, we measured field-cooled (FC) curves, as well as heat capacity curves in the absence of a magnetic field.

Figure 2(a) shows the results of the VSM magnetization versus field measurements of the Fe_5GeTe_2 sample, for temperatures ranging from 1.8 to 350 K, and external field applied along both the c-axis (dashed lines) and the ab-plane (solid lines) directions. The curves show that the easy-axis of Fe_5GeTe_2

is in-plane because a stronger field is required to saturate the sample along the c-axis, compared to the abplane, at all temperatures. Further measurements (see supplementary material section I (available online at stacks.iop.org/2DM/8/045030/mmedia)) show that there is no uniaxial anisotropy within the ab-plane, establishing Fe₅GeTe₂ as an easy-plane magnet. Possible spin-reorientation features, such as the ones observed in Fe₄GeTe₂ [11], are not observed in this sample. Our results are reasonable considering the fact that the out-of-plane magnetocrystalline anisotropy in Fe₅GeTe₂ crystals is weak [11, 19]. Figure 2(b) shows the FC curves for the H||c| and the H||ab| cases. The magnetization magnitude change on the H||ab| curve indicates a possible magnetic phase transition. This feature has been reported in previous publications [11, 16, 19]. Based on the transition points of the FC curves, the Curie temperature was estimated to be $T_c = 332 \pm 5$ K.

Heat capacity measurements were used to validate the Curie temperature estimation. The measurements were set to start from the highest temperature setpoint, T = 390 K, then the temperature was gradually reduced to 1.8 K as the heat capacity data was collected. This procedure guarantees that an appropriate time constant is used to achieve more stable readings. The measurement results are shown in figure 2(c). Two points of interest are highlighted on the curve by two black arrows. The first is a transition at T = 332 K, which is consistent with T_c from the FC measurement. The second is the observation of a slope change around T = 110 K. The slope change again indicates that Fe₅GeTe₂ experiences some phase transition, which will be discussed more extensively in the analysis of FMR linewidth in section 4.

IOP Publishing 2D Mater. **8** (2021) 045030 L Alahmed *et al*

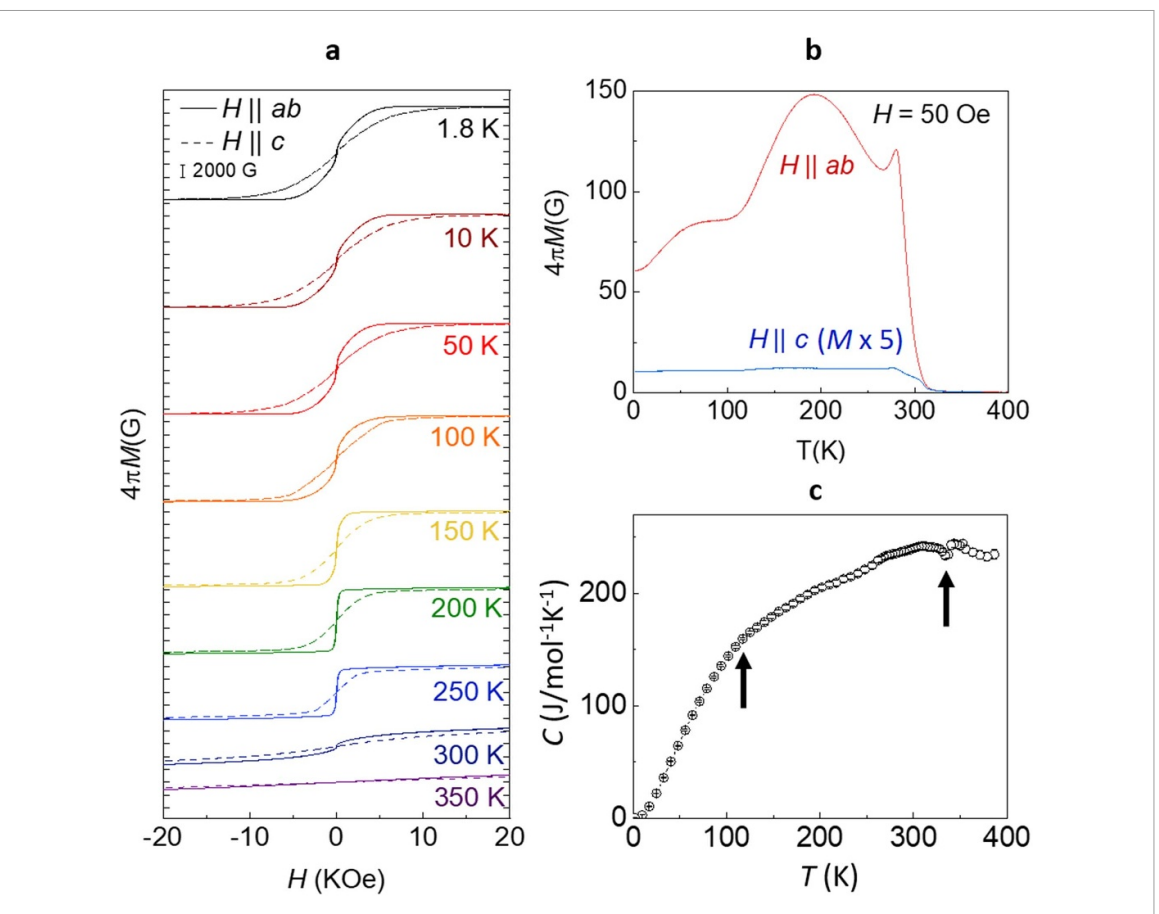


Figure 2. Static magnetization of the Fe₅GeTe₂ bulk single crystal. (a) Temperature-dependent hysteresis loops at various temperatures for H|c (dashed lines) and H|ab (solid lines). (b) FC curves (H=50 Oe) for the H|c (blue) and the H|ab (red) cases, respectively. (c) Heat capacity as a function of temperature. The transition at 332 and 110 K mark the Curie temperature and possible magnetic phase transition, respectively.

4. Magnetization dynamics

We measured the FMR response of the Fe₅GeTe₂ sample for H||c| and for H||ab|, at temperatures varying from 10 to 300 K. In our custom-built system, a coplanar waveguide with impedance matched to 50 Ω was used to guide the microwave field to the sample. The tested microwave frequencies ranged from 5 to 40 GHz, with higher frequencies up to 115 GHz used in the room temperature $H \parallel c$ case, along with high magnetic fields, to ensure that the magnetization of the sample is fully saturated at FMR. For each microwave frequency, the magnetic field was swept from high magnetic field toward zero. A microwave diode was used to convert the transmitted microwave signal to a dc voltage. To improve the signal-to-noise ratio, we used a set of field-modulation coils supplemented by a lock-in amplifier to detect the signal. Thus, the detected FMR response is identified as the derivative of microwave power absorption.

As shown in figure 3, we detected strong FMR responses at 300 K, demonstrating ferromagnetism of Fe₅GeTe₂ at room temperature. Figures 3(a) and (b) show the temperature dependence of the FMR profiles at 10 and 20 GHz, for H||c and H||ab, respectively. Besides the data points, the curves show fits

to the derivative of a combination of symmetric and antisymmetric Lorentzian functions [22]. The measured FMR response is a time-averaged signal of the microwave power absorption. Such absorption is dispersive and has a symmetric feature. However, there are a number of effects, including Eddy currents, that can lead to a phase shift of the driving microwave field relative to the original signal [28]. Such a phase shift leads to a quadrature component that manifests as an antisymmetric contribution to the FMR signal [29, 30]. From the fits, one can extract the resonance field H_r and peak-to-peak linewidth ΔH_{pp} as shown in figures 4 and 5, respectively. It is observed that the magnitude of the FMR peaks decays with reducing temperature in the H||c case. Below 200 K, the FMR signal becomes undetectable in this orientation. We attribute this phenomenon to the broadening of the FMR resonance peaks.

The resonance frequencies f vs. the FMR resonance fields H_r at different temperatures are plotted in figures 4(a) and (b) for the $H\|c$ and for the $H\|ab$ cases, respectively. The fitting equation for the $H\|c$ measurements is [31]:

$$f = \gamma' (H_r - 4\pi M_{\text{eff}}) \tag{2}$$

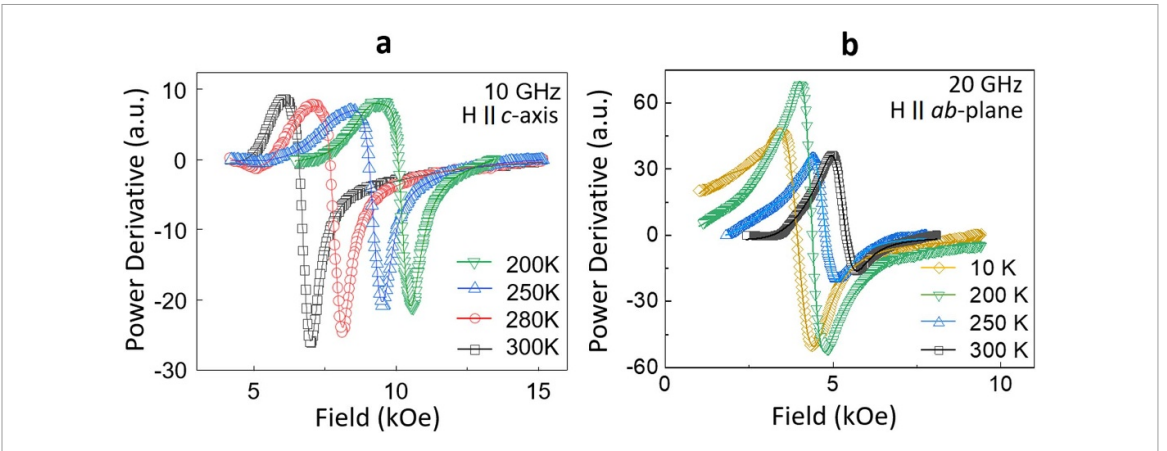


Figure 3. Ferromagnetic resonance (FMR) measurements of Fe₅GeTe₂ single crystal. (a) FMR profiles for $H \parallel c$ at 200, 250, 280, and 300 K. (b) FMR profiles for $H \parallel ab$ at 10, 200, 250 and 300 K.

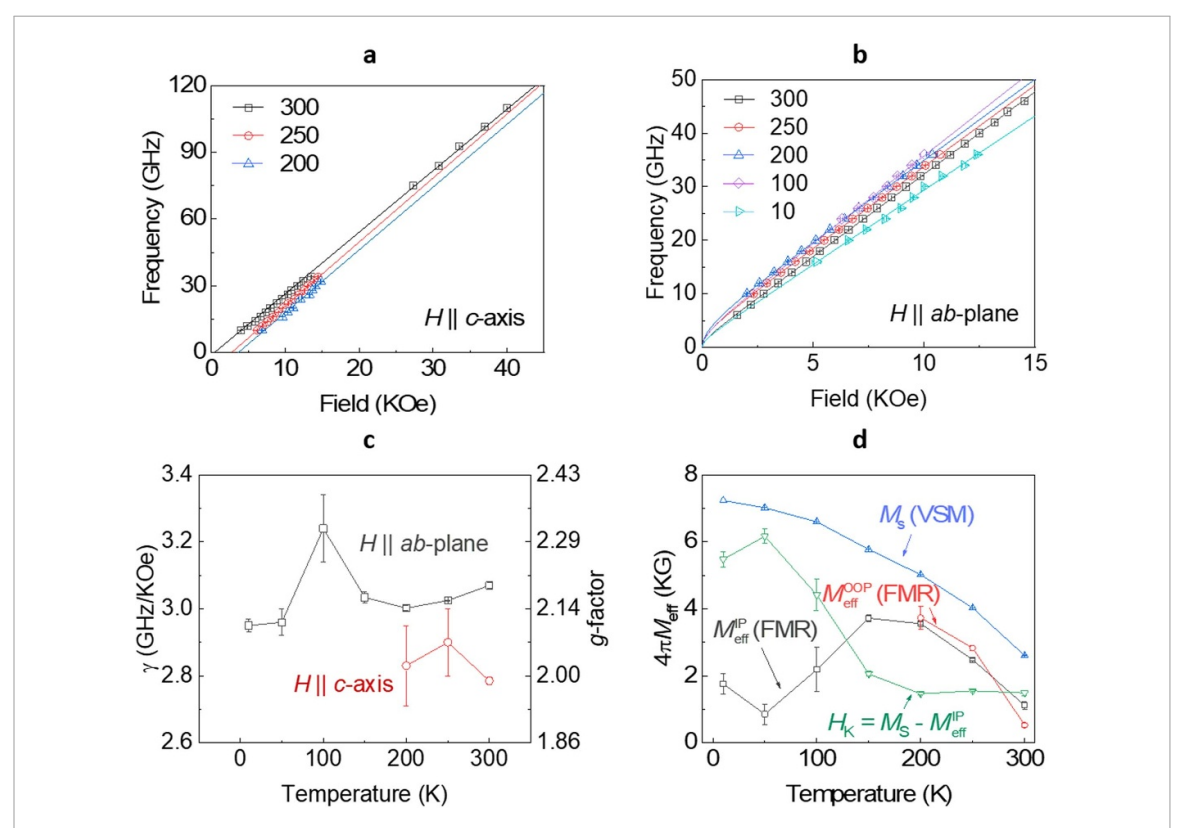


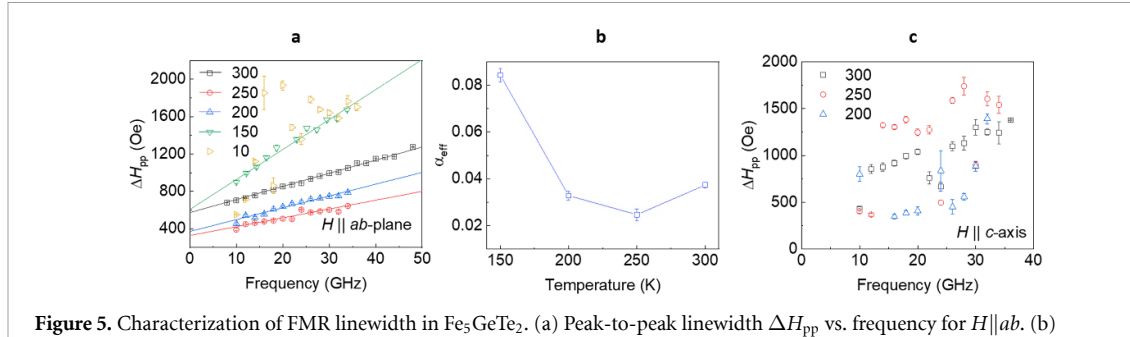
Figure 4. Analysis of the FMR data of the Fe₅GeTe₂ single crystal. (a) Frequency f vs. resonance field H_r at 200, 250, and 300 K for $H\|c$. The data points are fitted to equation (2). (b) Frequency f vs. resonance field H_r at 10, 100, 200, 250, and 300 K for $H\|ab$. The data points are fitted to equation (3). (c) Temperature dependence of the gyromagnetic ratio γ and spectroscopic g-factor for the $H\|c$ (red) and $H\|ab$ (black) cases, respectively. (d) Temperature dependence of saturation magnetization $4\pi M_s$ and effective magnetization $4\pi M_{eff}$ from VSM and FMR measurements, respectively.

and the fitting equation for the H||ab-plane measurements is [31]:

$$f = \gamma' \sqrt{(H_r + 4\pi M_{\text{eff}})H_r} \tag{3}$$

where f is frequency, γ' is the reduced gyromagnetic ratio ($\gamma' = \frac{|\gamma|}{2\pi}$), and $4\pi M_{\rm eff}$ is the effective magnetization. The fitted curves are also presented in figures 4(a) and (b). By fitting the data with equations (1) and (2), we obtain different γ' and corresponding

spectroscopic Landé g-factor values, as well as $M_{\rm eff}$ values, for the $H\|c$ and $H\|ab$ cases, as shown in figures 4(c) and (d), respectively. We note that the $4\pi M_{\rm eff}$ values obtained along those two orientations are in good agreement with each other. A difference between these two values could be an indication for the presence of a higher-order anisotropy [32], but this is not the case here. In figure 4(c), the left vertical axis shows γ' , and the right vertical axis shows the Landé g-factor calculated using $|\gamma| = g \frac{\mu_B}{\hbar}$. The



Temperature dependence of effective damping parameter $\alpha_{\rm eff}$ for $H \| ab$. (c) $\Delta H_{\rm pp}$ vs. frequency for $H \| c$.

g-factor exhibits a weak dependence on temperature along both the *ab*-plane and the *c*-axis directions. However, it deviates from g = 2 for both directions.

Furthermore, our data appear to indicate a sizable difference of the g-factor along different directions in Fe₅GeTe₂. Similar to Cr₂Ge₂Te₆ [26], the deviation of the g-factor from g = 2 may suggest an orbital contribution to the magnetization due to spin-orbit coupling in Fe₅GeTe₂. It was found that strong spinorbit coupling results in nontrival Berry phase in Fe₃GeTe₂, another member in the Fe_nGeTe₂ $(n \ge 3)$ family. In this case, the orbital character is formed by a mixture of 3D orbitals from the Fe I-Fe I dumbbells and Fe II sites [33]. A theoretical work found that the magnons can have long lifetimes and exhibit nonreciprocal magnon transport in Fe₃GeTe₂ [34]. In Fe₅GeTe₂, the spin-orbit coupling could be characterized by the d orbitals of Fe atoms and p orbitals of Te atoms [26]. In addition, the anisotropy of the g-factor, which follows from that of the orbital moment, is also expected physically: a small orbital moment arising from reduced crystalline symmetry may 'lock' the large isotropic spin moment into its favorable lattice orientation through spin-orbit coupling, giving rise to a sizable magnetic anisotropy. Therefore, it is likely that the orbital moment is closely linked to the magnetocrystalline anisotropy in itinerant ferromagnets, as shown theoretically by Bruno [35] for transitionmetal monolayers. Moreover, a recent experiment used x-ray magnetic circular dichroism and detected the contribution of the orbital moment to the overall magnetization of Fe₅GeTe₂ [18].

It is worth noting that an unsaturated magnetization at FMR can also lead to an inaccurate estimation of the gyromagnetic ratio [36]. Because the c-axis magnetization saturates at significantly larger magnetic fields, it is possible that the magnetization was not fully saturated for FMR measurements up to 40 GHz. To estimate to first order the influence of an unsaturated sample at resonance, we write $4\pi M_{\rm eff}(H) = 4\pi M_{\rm eff,0} + 4\pi pH$, where H is the external field, $4\pi M_{\text{eff,0}}$ is the effective magnetization extrapolated to zero field, and $4\pi p$ is the slope of $4\pi M_{\rm eff}$ vs. H curve in the region where FMR occurs. Using this equation, equation (2) can be

written as: $f = \gamma'_{\text{meas}}(H_r - 4\pi M_{\text{eff,meas}})$, with $\gamma'_{\text{meas}} =$ $\gamma'(1-4\pi p)$ and $4\pi M_{\rm eff,meas} = \frac{4\pi M_{\rm eff}}{1-4\pi p}$. To exclude this possibility and to confirm the g-factor anisotropy, we used a high-frequency, high-magnetic-field setup for the FMR measurement (supplementary material section III). The resulting *g*-factor extracted from the high-field FMR data still shows a significant difference between the ab-plane and c-axis, as shown in figure 4(c). Thus, the data support the presence of a g-factor anisotropy in Fe₅GeTe₂.

The fits also yield the effective magnetization $4\pi M_{\rm eff}$ at different temperatures. Figure 4(d) plots $4\pi M_{\rm eff}$ for both $H\|c$ (i.e. $4\pi M_{\rm eff}^{H\|c}$) and $H\|ab$ (i.e. $4\pi M_{eff}^{H\parallel ab}$) cases measured from FMR, along with the saturation magnetization $4\pi M_s$ measured from VSM. One can see (1) $4\pi M_{\rm eff}^{H\parallel c}$ and $4\pi M_{\rm eff}^{H\parallel ab}$ are close, and (2) there is a difference between $4\pi M_s$ and $4\pi M_{\rm eff}$. This reveals a crystalline anisotropy field that can be calculated by $H_{\rm k}=4\pi M_{\rm s}$ — $4\pi M_{\rm eff}^{\dot{H}\parallel ab}$. As plotted in figure 4(d), H_k is positive and reduces with increasing temperature. This shows that there exists an out-ofplane crystalline anisotropy field H_k of several kOe, though it is smaller than the in-plane shape anisotropy. This observation is consistent with previous reports [11, 19].

Next, we analyze the FMR linewidth in order to gain insights into the spin scattering mechanisms in Fe₅GeTe₂. In figures 5(a) and (c), we plot the peak-to-peak linewidth $\Delta H_{\rm pp}$ vs. frequency at different temperatures measured for the H||ab| and the H||c cases, respectively. For an ideal magnetic thin film that is homogeneous and defect-free, the linewidth reflects intrinsic FMR damping. In this scenario, the uniform magnon mode (k = 0, ferromagnetic resonance) decays into Stoner excitations as temperature decreases. This involves the transition of an electron from an occupied state to an unoccupied state of the same wave-vector, which can be described by the interband term in Kambersky's formula [37, 38]. It should be noted that Kambersky's model is only appropriate to second order in spinorbit coupling parameter ξ , but to higher order no intraband terms occur [39]. Besides intrinsic damping, due to non-uniform magnetization states and defects in the sample, the linewidth can be broadened

2D Mater. 8 (2021) 045030 L Alahmed et al

Table 1. Summary of measured effective Gilbert damping constants for different materials at different temperatures.

Material	Туре	Gilbert damping constant	Temperature (K)	Source
NiFe (permalloy) thin	3D-conducting	0.013	300	Reference [43]
film (3 nm)				
Fe ₅ GeTe ₂	2D-conducting	0.035	300	This work
Fe ₅ GeTe ₂	2D-conducting	0.007	10	This work
CrBr ₃	2D-insulating	0.009	30	Reference [44]
Cr ₂ Ge ₂ Te ₆	2D-insulating	0.01-0.08	10	Reference [27]

by extrinsic scattering mechanisms such as inhomogeneous line broadening ΔH_0 and two-magnon scattering $\Delta H_{\rm TMS}$. Thus, the FMR linewidth $\Delta H_{\rm pp}$ can be expressed by the following form [40]:

$$\Delta H_{\rm pp} = \frac{2\alpha_{\rm eff}}{\sqrt{3}|\gamma|} \frac{f}{2\pi} + \Delta H_0 + \Delta H_{\rm TMS}. \tag{4}$$

Figures 5(a) and (c) plot the FMR linewidth versus frequency for H||ab| and H||c| cases, respectively. We measured linewidths with the magnitude between 400 and 2000 Oe for both cases. As shown in figure 5(a), the FMR linewidth increases when the temperature reduces from 300 to 150 K. The linewidth becomes higher and very scattered below 150 K. This indicates extrinsic contributions in Fe₅GeTe₂ at lower temperatures. A previous study showed that when FeRh transitions from ferromagnetic to antiferromagnetic, it exhibits a significant increase of the FMR linewidth [41]. Other studies have shown a significant increase of the linewidth in magnetite as it undergoes the Verwey transition [42]; the effective damping increases in Py/Gd bilayers when approaching the Gd ordering temperature [36]. It is likely that the increased linewidth we have observed can also arise from similar magnetic phase transitions. In fact, Zhang et al [19] has proposed that Fe₅GeTe₂ transitions from ferromagnetic to ferrimagnetic at 275 K, and then transitions to a state with glassy clusters below 110 K. While our AC susceptibility results show no indication of a state with glassy clusters (supplementary material section II), our lowtemperature FMR measurements support the argument of ferromagnetic to ferrimagnetic transitions at lower temperatures. We acknowledge that Fe₅GeTe₂ has very intriguing and complex magnetism and we believe that a complete understanding will require many further studies.

The FMR measurements have shown that Fe_5GeTe_2 exhibits a similar damping constant to that of soft 3D magnets, when interpreting the slope of the linewidth as an effective Gilbert damping parameter. As can be seen from figure 5(b), the effective damping parameter α_{eff} ranges from 0.025 to 0.085 as temperature reduces from 300 to 150 K. We summarized table 1 for a comparison of the Gilbert damping constant for typical materials. It can be seen that the reported vdW magnets have similar damping constants as 3D magnets. The α_{eff} of Fe_5GeTe_2 is similar

to that of soft 3D transition metal magnets such as Permalloy [43]. Because $\alpha_{\rm eff}$ of Fe₅GeTe₂ is estimated from the $H\|ab$ measurements, it is likely that $\Delta H_{\rm TMS}$ also contributes to $\alpha_{\rm eff}$.

5. Summary and conclusion

In summary, we have synthesized a vdWs Fe₅GeTe₂ crystal that showed a bulk Curie temperature of 332 K. While the Curie temperature of Fe₅GeTe₂ is expected to decrease when the vdWs crystal is exfoliated into thin layers, the bulk value is still one of the highest recorded for a vdWs bulk magnet until now, making it an attractive 2D option to be used in spintronic devices. We used both VSM and FMR to study the magnetic properties of the Fe₅GeTe₂ sample. The experiments were performed with external magnetic fields applied along the c-axis and the ab-plane directions from 300 to 10 K. We have focused on the temperature and field dependences of the g-factor and spin scattering mechanisms. The g-factor along the ab-plane is larger than that along the c-axis, indicative of considerable orbital momentum arising from spin-orbit coupling in Fe₅GeTe₂. The FMR analysis also reveals low temperature-enhanced linewidth broadening, together with the VSM data, they indicate a ferromagnetic to ferrimagnetic transition at lower T. For future studies, it will be interesting to exploit Fe₅GeTe₂ thin films for spin transport and spin-to-charge conversion experiments at room temperature. Fe₅GeTe₂ also opens new ways to build and study hybrid magnonic structures.

Acknowledgments

L A acknowledges the U.S. National Science Foundation (NSF) under grant No. DMR-2129879335 and Auburn University Research Support Program. L B is supported by the US DOE, Basic Energy Sciences program through Award DE-SC0002613. A portion of this work was performed at the National High Magnetic Field Laboratory, which is supported by the National Science Foundation Cooperative Agreement No. DMR-1644779 and the State of Florida. A R M and M B are supported by the U.S. Department of Energy, Office of Science, Basic Energy Sciences, Materials Sciences and Engineering Division. B N acknowledges support through NSF MEMONET

Grant #1939999, A S acknowledges support NSF-CAREER Award #1452670, Work by S S-L Z was supported by the College of Arts and Sciences, Case Western Reserve University, and P L acknowledges the Ralph E Powe Junior Faculty Enhancement Award and valuable discussions with Prof Mingzhong Wu, Prof Satoru Emori, Prof Wei Zhang, Dr. Chuanjun Liu. L A acknowledges Dr. Kaya Wei for providing the single crystal x-ray data.

Data availability statement

All data that support the findings of this study are included within the article (and any supplementary files).

ORCID iDs

Laith Alahmed 6 https://orcid.org/0000-0001-8214-7118

Masoud Mahjouri-Samani https://orcid.org/0000-0002-6080-7450

Luis Balicas https://orcid.org/0000-0002-5209-0293

Peng Li https://orcid.org/0000-0001-8491-0199

References

- [1] Frisenda R, Niu Y, Gant P, Muñoz M and Castellanos-Gomez A 2020 Naturally occurring van der Waals materials npj 2D Mater. Appl. 4 38
- [2] Mak K F, Shan J and Ralph D C 2019 Probing and controlling magnetic states in 2D layered magnetic materials *Nat. Rev. Phys.* 1 646–61
- [3] Mitta S B, Choi M S, Nipane A, Ali F, Kim C, Teherani J T, Hone J and Yoo W J 2020 Electrical characterization of 2D materials-based field-effect transistors 2D Mater. 8 012002
- [4] Casto L D et al 2015 Strong spin-lattice coupling in CrSiTe₃ APL Mater. 3 041515
- [5] Carteaux V, Brunet D, Ouvrard G and Andre G 1995 Crystallographic, magnetic and electronic structures of a new layered ferromagnetic compound Cr₂Ge₂Te₆ J. Phys.: Condens. Matter. 7 69–87
- [6] Tsubokawa I 1960 On the magnetic properties of a CrBr₃ single crystal I. Phys. Soc. Japan 15 1664–8
- [7] McGuire M A, Dixit H, Cooper V R and Sales B C 2015 Coupling of crystal structure and magnetism in the layered, ferromagnetic insulator CrI₃ Chem. Mater. 27 612–20
- [8] Deiseroth H-J, Aleksandrov K, Reiner C, Kienle L and Kremer R K 2006 Fe3GeTe2 and Ni3GeTe2—two new layered transition-metal compounds: crystal structures, HRTEM investigations and magnetic and electrical properties Eur. J. Inorg. Chem. 2006 1561–7
- [9] Chen B, Yang J, Wang H, Imai M, Ohta H, Michioka C, Yoshimura K and Fang M 2013 Magnetic properties of layered itinerant electron ferromagnet Fe₃GeTe₂ J. Phys. Soc. Japan 82 124711
- [10] Bander M and Mills D L 1988 Ferromagnetism of ultrathin films Phys. Rev. B 38 12015–18
- [11] Seo J et al 2020 Nearly room temperature ferromagnetism in a magnetic metal-rich van der Waals metal Sci. Adv. 6 eaay8912
- [12] Deng Y et al 2018 Gate-tunable room-temperature ferromagnetism in two-dimensional Fe₃GeTe₂ Nature 563 94–9

- [13] Li Z et al 2020 Magnetic critical behavior of the van der Waals Fe₅GeTe₂ crystal with near room temperature ferromagnetism Sci. Rep. 10 15345
- [14] Zhu J-X et al 2016 Electronic correlation and magnetism in the ferromagnetic metal Fe₃GeTe₂ Phys. Rev. B 93 144404
- [15] Verchenko V Y, Tsirlin A A, Sobolev A V, Presniakov I A and Shevelkov A V 2015 Ferromagnetic order, strong magnetocrystalline anisotropy and magnetocaloric effect in the layered telluride Fe₃₋₆GeTe₂ Inorg. Chem. 54 8598–607 PMID: 26267350
- [16] May A F et al 2019 Ferromagnetism near room temperature in the cleavable van der Waals crystal Fe₅GeTe₂ ACS Nano 13 4436–42
- [17] May A F, Bridges C A and McGuire M A 2019 Physical properties and thermal stability of Fe_{5-x}GeTe₂ single crystals *Phys. Rev. Mater.* 3 104401
- [18] Yamagami K et al 2021 Itinerant ferromagnetism mediated by giant spin polarization of the metallic ligand band in the van der Waals magnet Fe₅GeTe₂ Phys. Rev. B 103 L060403
- [19] Zhang H et al 2020 Itinerant ferromagnetism in van der Waals Fe_{5-x} GeTe₂ crystals above room temperature *Phys. Rev.* B **102** 064417
- [20] Gao Y et al 2020 (Anti)meron chains in the domain Walls of van der Waals ferromagnetic Fe_{5-x}GeTe₂ Adv. Mater. 32 2005228
- [21] Ohta T, Sakai K, Taniguchi H, Driesen B, Okada Y, Kobayashi K and Niimi Y 2020 Enhancement of coercive field in atomically-thin quenched Fe₅GeTe₂ Appl. Phys. Express 13 043005
- [22] Oates C, Ogrin F, Lee S, Riedi P, Smith G and Thomson T 2002 High field ferromagnetic resonance measurements of the anisotropy field of longitudinal recording thin-film media J. Appl. Phys. 91 1417–22
- [23] Shaw J M, Nembach H T, Silva T J and Boone C T 2013 Precise determination of the spectroscopic g-factor by use of broadband ferromagnetic resonance spectroscopy J. Appl. Phys. 114 243906
- [24] Lee I, Utermohlen F G, Weber D, Hwang K, Zhang C, van Tol J, Goldberger J E, Trivedi N and Hammel P C 2020 Fundamental spin interactions underlying the magnetic anisotropy in the Kitaev ferromagnet CrI₃ Phys. Rev. Lett. 124 017201
- [25] Zeisner J, Mehlawat K, Alfonsov A, Roslova M, Doert T, Isaeva A, Büchner B and Kataev V 2020 Electron spin resonance and ferromagnetic resonance spectroscopy in the high-field phase of the van der Waals magnet CrCl₃ Phys. Rev. Mater. 4 064406
- [26] Khan S, Zollitsch C W, Arroo D M, Cheng H, Verzhbitskiy I, Sud A, Feng Y P, Eda G and Kurebayashi H 2019 Spin dynamics study in layered van der Waals single-crystal Cr₂Ge₂Te₆ Phys. Rev. B 100 134437
- [27] Zhang T, Chen Y, Li Y, Guo Z, Wang Z, Han Z, He W and Zhang J 2020 Laser-induced magnetization dynamics in a van der Waals ferromagnetic Cr₂Ge₂Te₆ nanoflake Appl. Phys. Lett. 116 223103
- [28] Flovik V, Macià F, Kent A D and Wahlström E 2015 Eddy current interactions in a ferromagnet-normal metal bilayer structure and its impact on ferromagnetic resonance lineshapes J. Appl. Phys. 117 143902
- [29] Harder M, Cao Z X, Gui Y S, Fan X L and Hu C-M 2011 Analysis of the line shape of electrically detected ferromagnetic resonance *Phys. Rev.* B 84 054423
- [30] Mecking N, Gui Y S and Hu C-M 2007 Microwave photovoltage and photoresistance effects in ferromagnetic microstrips Phys. Rev. B 76 224430
- [31] Chang H, Li P, Zhang W, Liu T, Hoffmann A, Deng L and Wu M 2014 Nanometer-thick yttrium iron garnet films with extremely low damping *IEEE Magn. Lett.* 5 1–4
- [32] Rai A, Sapkota A, Pokhrel A, Li M, De Graef M, Mewes C, Sokalski V and Mewes T 2020 Higher-order perpendicular magnetic anisotropy and interfacial damping of Co/Ni multilayers *Phys. Rev.* B 102 174421

2D Mater. 8 (2021) 045030 L Alahmed et al

[33] Kim K et al 2018 Large anomalous Hall current induced by topological nodal lines in a ferromagnetic van der Waals semimetal Nat. Mater. 17 794–9

- [34] Costa M, Peres N M R, Fernández-Rossier J and Costa A T 2020 Nonreciprocal magnons in a two-dimensional crystal with out-of-plane magnetization *Phys. Rev.* B 102 014450
- [35] Bruno P 1989 Tight-binding approach to the orbital magnetic moment and magnetocrystalline anisotropy of transition-metal monolayers *Phys. Rev.* B 39 865–8
- [36] Khodadadi B, Mohammadi J B, Mewes C, Mewes T, Manno M, Leighton C and Miller C W 2017 Enhanced spin pumping near a magnetic ordering transition *Phys. Rev.* B 96 054436
- [37] Spin-orbital K V 2007 Gilbert damping in common magnetic metals Phys. Rev. B 76 134416
- [38] Edwards D M 2016 The absence of intraband scattering in a consistent theory of Gilbert damping in pure metallic ferromagnets J. Phys.: Condens. Matter 28 086004

- [39] Costa A T and Muniz R B 2015 Breakdown of the adiabatic approach for magnetization damping in metallic ferromagnets *Phys. Rev.* B 92 014419
- [40] Jiang S, Sun L, Yin Y, Fu Y, Luo C, Zhai Y and Zhai H 2017 Ferromagnetic resonance linewidth and two-magnon scattering in $\mathrm{Fe_{1-x}Gd_x}$ thin films AIP Adv. 7 056029
- [41] Wang Y et al 2020 Spin pumping during the antiferromagnetic–ferromagnetic phase transition of iron–rhodium Nat. Commun. 11 275
- [42] Srivastava A, Singh A V, Mohammadi J B, Mewes C, Gupta A and Mewes T 2020 Ferromagnetic resonance study of the verwey phase transition of magnetite thin film on MgGa₂O₄(001) substrate *IEEE Trans. Magn.* 56 1–6
- [43] Zhao Y, Song Q, Yang S-H, Su T, Yuan W, Parkin S S P, Shi J and Han W 2016 Experimental investigation of temperature-dependent gilbert damping in permalloy thin films Sci. Rep. 6 22890
- [44] Shen X et al 2021 Multi-domain ferromagnetic resonance in magnetic van der Waals crystals CrI₃ and CrBr₃ J. Magn. Magn. Mater. 528 167772